Journal of Chromatography, 461 (1989) 103–110
Elsevier Science Publishers B.V., Amsterdam — Printed in The Netherlands

CHROM. 1413

SEDIMENTATION FIELD-FLOW FRACTIONATION OF COLLOIDAL METAL HYDROSOLS

LARRY E. OPPENHEIMER* and GREGORY A. SMITH
Photographic Research Laboratories, Photographic Products Group, Eastman Kodak Company, Rochester, NY 14650 (U.S.A.).

SUMMARY

Sedimentation field-flow fractionation can be readily used to characterize the particle size distributions in metal hydrosols with particle diameters extending well below 0.01 μm. Processes that change the size distribution, such as particle growth or coagulation, can be investigated by this method. For materials such as silver, where the optical properties of the hydrosol depend on the particle shape, sedimentation field-flow fractionation can be combined with detection by diode array spectrophotometry to obtain data that allow inferences to be made about the non-spherical nature of the dispersed material.

INTRODUCTION

Dispersions of metal particles in aqueous media have been investigated by colloid chemists for many years. A century ago Carey Lea[1] described procedures that are still in use for producing silver hydrosols. Recently there has been an increase in interest in these sols because of their utility as substrates for surface-enhanced Raman scattering experiments. As with other uses for colloidal systems, the relevant properties of the sol depend on the size, shape, and/or specific surface area of the metal particles[2]. Jolivet *et al.*[3] demonstrated that silver sols are subject to particle growth and aggregation when no protective colloid is present. Characterization of these materials has generally been done by electron microscopy. Unfortunately, the information about the state of aggregation of a sol contained in micrographs is often ambiguous because it is difficult to tell if the sample has been aggregated, or deaggregated, in preparation for microscopy. Also, quantitative information about systems of non-spherical particles is difficult to obtain by electron microscopy. In a recent publication[4] we described the use of sedimentation field-flow fractionation (SFFF) for the characterization of particle size distributions in metal sols containing both spherical and filamentary particles and have found it to be both fast and accurate as well as sensitive to the state of aggregation of the sample.

While measurement of the distribution of particle masses, or diameters for spherical particles, by SFFF is straightforward, obtaining shape information about sols containing non-spherical particles is much more difficult. An example of such a

system is filamentary silver, which is often the product of photographic development of silver halide particles[5]. SFFF allows the separation of particles from a dispersion of silver filaments according to their mass without regard to particle shape[6]. Detection with a diode array spectrophotometer can then be used to generate spectra of the effluent of the SFFF system. The results are a series of spectra for fractions of increasing particle mass. The spectra of silver particles vary considerably with the axial ratio of the particles[2,7]. This property makes it possible to derive particle shape information from the fractogram and spectra. Similarly, silver spheres in the early stages of aggregation have the optical properties of ellipsoids and show the optical effects of non-spherical particles[2].

EXPERIMENTAL

Instrumentation

Separations were performed on a SF[3]1000 particle fractionator produced by the Clinical & Instrument Systems Division of DuPont (Wilmington, DE, U.S.A.). The device has a 0.025-cm channel width and an integral DuPont Instruments 860 absorbance detector that was operated at 254 nm. It is similar to devices described in the literature[8]. Experiments were performed using a time-delayed exponential-decay programmed field[8,9] with initial rotor speeds between 10 000 and 15 000 rpm, which correspond to fields of 10 647 and 23 957 *g*, respectively. In all experiments the field decay constant was 4 min, the relaxation time was 2 min, and the flow-rate was 2 ml/min. A 0.1% aqueous solution of FL-70 surfactant (Fischer Scientific, Fair Lawn, NJ, U.S.A.) was used as the eluent.

Spectra were obtained with an HP 8452 diode array spectrophotometer (Hewlett Packard, Palo Alto, CA, U.S.A.) equipped with a 30-μl flow cell. Typically, spectra were collected at 2-min intervals during peak elution over the wavelength range 300–820 nm.

Dispersions

Filamentary silver was made by photographic development of chemically fogged silver halide in gelatin[5]. An electron micrograph of such a sol appears in Fig. 1.

Silver sols containing spherical particles were made by reduction of silver oxide with dextrin or by the reduction of silver nitrate with iron(II) sulfate in the presence of sodium citrate[10–12]. For storage, 10% (by weight) gelatin was added to the dispersions.

RESULTS

The output of the SFFF system for each experiment, a curve of extinction *versus* time, was used to generate a particle size distribution by applying an equation of the form $t = 3\tau \ln (D / \beta)$ to the time axis[9]. This relationship between elution time t and D, the diameter for spherical particles or equivalent spherical diameter for non-spherical particles, is valid for time-delayed exponential-decay programmed field SFFF when t is greater than the time constant for rotor speed decay, τ. Here β contains the sample and eluent densities and instrumental parameters. The absorb-

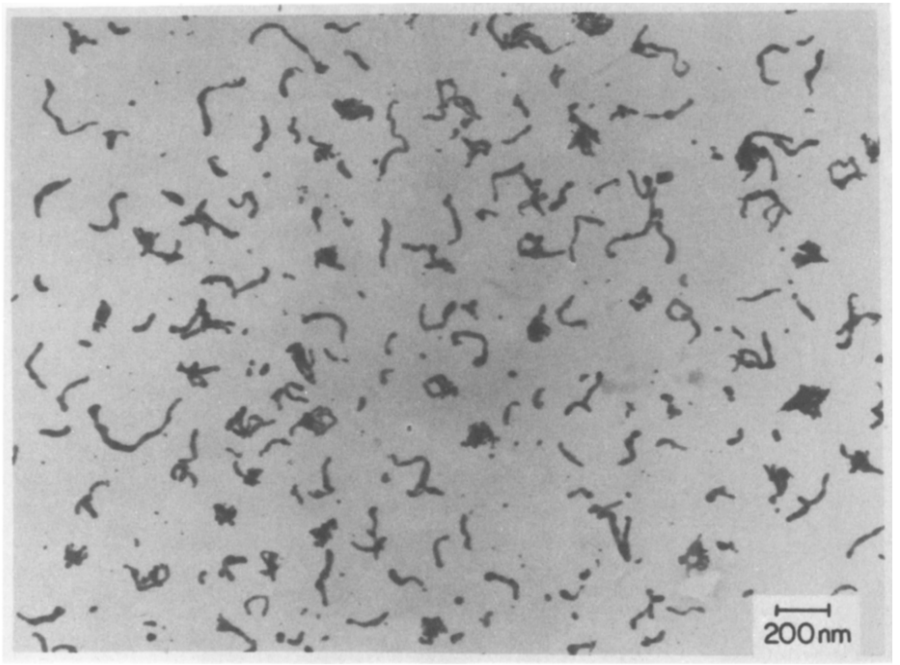

Fig. 1. Electron micrograph of particles in a filamentary silver sol.

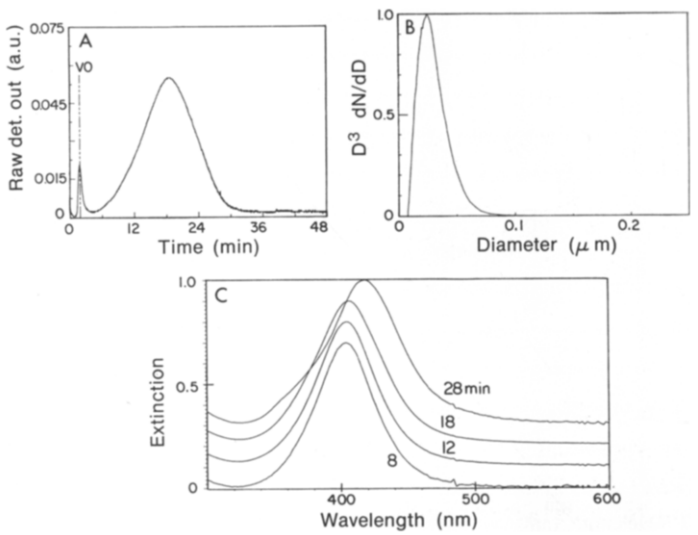

Fig. 2. Results for a sol containing spherical silver particles that were stabilized with gelatin. (A) Raw SFFF data. (B) Particle size distribution. (C) Spectra taken of the eluent at the indicated elution times (*cf.* A).

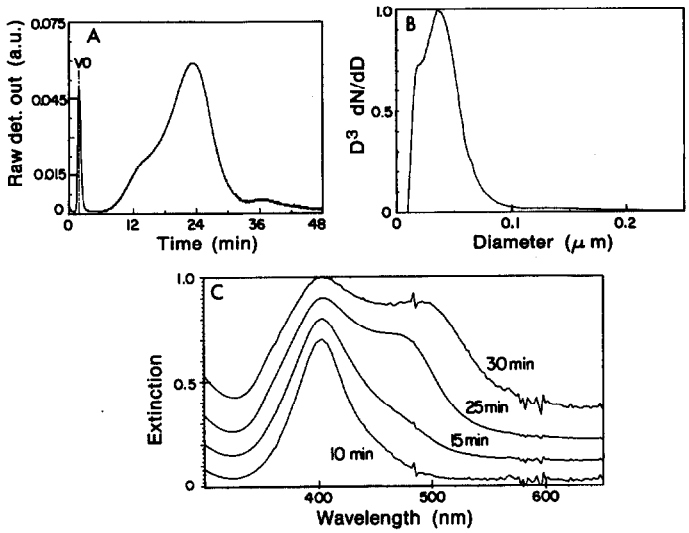

Fig. 3. Results for the sol described in Fig. 2 after coagulation. (A) Raw SFFF data. (B) Particle size distribution. (C) Spectra taken of the eluent at the indicated elution times (*cf.* A).

ance at each time was related to the mass frequency of particles by dividing by the calculated diameter, as explained in our earlier paper[4], to yield a value proportional to $D^3\ dN/dD$. In this manner a mass distribution was obtained for each sample. The raw data and corresponding size distributions are shown in Fig. 2A and B–4A and B. In addition, four of the spectra obtained in the course of each experiment, normalized to the same height in each case, are included in Figures 2C–4C.

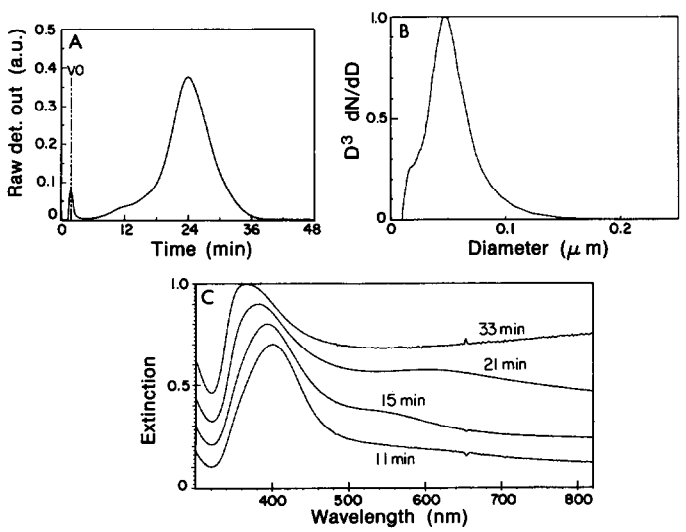

Fig. 4. Results for a sol containing filamentary silver particles that were stabilized with gelatin. (A) Raw SFFF data. (B) Particle size distribution. (C) Spectra taken of the eluent at the indicated elution times (*cf.* A).

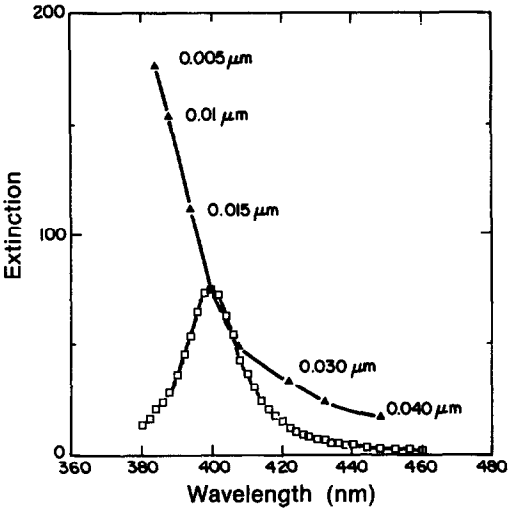

Fig. 5. Calculated extinction spectrum for 0.02 μm silver spheres (□) and the locus of the peak positions as a function of particle diameter (▲).

DISCUSSION

Optical absorption by colloidal dispersions of silver is known to depend on both the size and shape of the dispersed particles[2,7]. The extinction spectra of these materials are, in principle, readily calculated using the Mie equations for spherical particles or the Rayleigh-Gans approximation for ellipsoidal particles (see ref. 13). However, the calculations require a knowledge of the complex refractive index of the particles as a function of wavelength. There are several sets of refractive index data for silver in the literature, with significant variations among them[14]. We have chosen to use the data of Johnson and Christy[15] because they give a clear indication of the

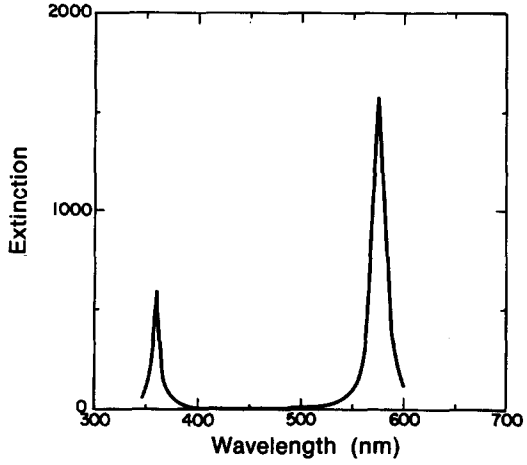

Fig. 6. Calculated extinction spectrum for silver ellipsoids with minor axis 0.02 μm and axial ratio 3.0.

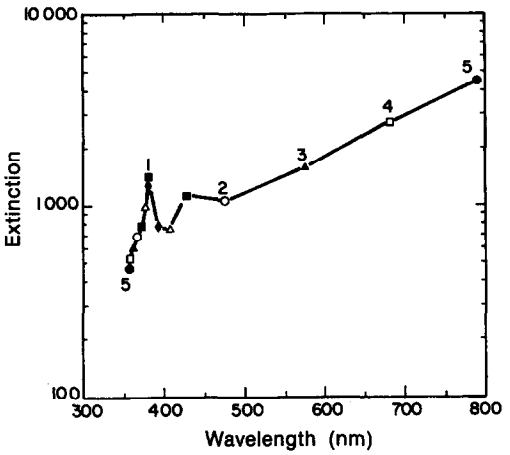

Fig. 7. Locus of peak positions calculated for extinction by silver ellipsoids with minor axis 0.02 μm as a function of axial ratio.

trends we expect to find as the particle size and shape vary and they have been used by other investigators for similar studies.

Fig. 5 shows the extinction behavior of spherical silver particles as a function of diameter. The spectrum is shown for particles 0.02 μm in diameter along with the locus of the peak extinction for varying diameter. Note that the peak moves to longer wavelengths as the diameter increases. When we consider ellipsoidal particles, we find that the extinction spectrum splits into two peaks, as shown in Fig. 6 for an axial ratio of 3.0. The locus of the peaks is plotted as a function of axial ratio in Fig. 7 for constant minor axis of 0.02 μm. The long wavelength peak moves to longer wavelengths and the short wavelength peak to shorter wavelengths as the axial ratio increases with the minor axis held constant. Kerker[2] reported similar results for calcu-

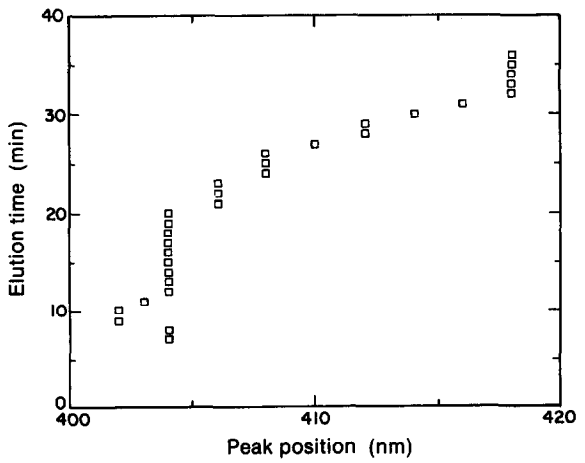

Fig. 8. Peak position as a function of elution time for SFFF of the silver sol containing spherical particles.

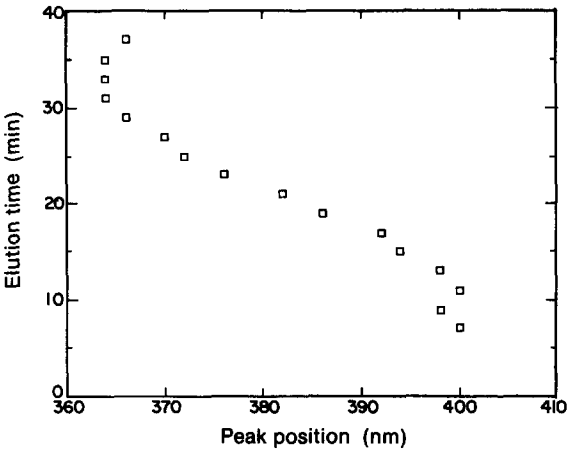

Fig. 9. Position of the short wavelength peak as a function of elution time for SFFF of the silver sol containing filamentary particles.

lations performed for particles at different axial ratios with the particle volume held constant. The changes in peak position and magnitude predicted in these graphs can be observed experimentally, while the peaks are broader than predicted by the Rayleigh-Gans theory.

Given this background we can attempt to understand the results of SFFF with diode array detection on three different samples samples of colloidal silver. Fig. 2 contains results for a sample of spherical colloidal silver protected from aggregation by absorbed gelatin. We have shown earlier[4] that the gelatin itself has no effect on the SFFF results. The spectra are similar, the main feature being a single peak close to 400 nm. As predicted in Fig. 5, the position of the peak moves to longer wavelengths as the particle size increases while the peak shape remains unchanged. The peak position is plotted as a function of elution time in Fig. 8. The discontinuous appearance of this plot, and of Fig. 9, is due in large measure to the limited wavelength resolution of the diode array detection, 2 nm in our case.

Fig. 3 contains SFFF results and spectra for a sample of the same sol which had been destabilized by the addition of a proteolytic enzyme 1 h prior to the experiment. The enzyme destroyed the gelatin, allowing the particles to aggregate. On visual observation it was noted that the color of the sol changed from yellow to red-orange. The particle size distribution has changed in the manner we might expect for an aggregating sol, with a shoulder remaining at small particle sizes corresponding to the original, unaggregrated, particles as well as the appearance of a shoulder at larger sizes corresponding to the appearance of large particles, *i.e.*, aggregates. The spectra clearly reflect the ellipsoid-like behavior of these particles. For the smaller particles the spectra are similar to those in Fig. 2. As larger particles were examined, a shoulder formed on the long wavelength side of the peak, which eventually evolved into a distinct, if poorly resolved, second peak. The wavelength of the second maximum is somewhat less than 500 nm, as predicted for ellipsoids with an axial ratio of about 2. We expect this since the main cause of the peak is most likely the presence of doublets in the dispersion. The position of the short wavelength peak is constant across the

fractogram, showing neither the shift to longer wavelengths associated with increasingly large spherical particles or the shift to shorter wavelengths of ellipsoids. This is probably the result of a fortuitous combination of both these phenomena occurring simultaneously.

Fig. 4. contains the results for a filamentary silver sol. The results are not nearly as dramatic as those in Fig. 3, but the formation of the second peak, which moves to longer wavelengths as the particle mass increases, can be seen. The position of this peak is beyond the 820 nm limit of our detector for the largest particles present here. For this sample, where there are relatively few spherical particles, the short wavelength peak does move to shorter wavelengths as the particle mass increases, as shown in Fig. 9. The broadness of the peak for this sample is not unexpected because of the polydispersity of the sample with respect to axial ratio and the wide deviations from ellipsoidal particle shape of some of the particles.

In conclusion then, SFFF can be used to determine particle size (or mass) distributions in metal hydrosols without regard to the particle shape. When combined with spectrophotometric detection using a diode array detector, SFFF can be used to obtain particle shape information for dispersions of non-spherical particles when the absorption spectrum of the dispersed phase is a function of the particle shape. We have demonstrated this using silver dispersions consisting of unaggregated and aggregated spherical particles and of filamentary particles.

REFERENCES

1 M. Carey Lea, *Am. J. Sci.*, 37 (1889) 476.
2 M. Kerker, *J. Colloid Interface Sci.*, 105 (1985) 297.
3 J.P. Jolivet, M. Gzara, J. Mazieres and J. Lefebvre, *J. Colloid Interface Sci.*, 107 (1985) 429.
4 L.E. Oppenheimer and G.A. Smith, *Langmuir*, 4 (1987) 144.
5 T.H. James (Editor), *The Theory of the Photographic Process*, Macmillan, New York, 4th ed., 1977.
6 J.J. Kirkland, L.E. Schallinger and W.W. Yau, *Anal. Chem.*. 57 (1985) 2271.
7 D.C. Skillman and C.R. Berry, *J. Chem. Phys.*, 48 (1968) 3297.
8 J.J. Kirkland, S.W. Rementer and W.W. Yau, *Anal. Chem.*, 53 (1981) 1730.
9 W.W. Yau and J.J. Kirkland, *Sep. Sci.*, 16 (1981) 577.
10 G. Frens and J.Th.G. Overbeek, *Kolloid-Z.*, 233 (1969) 922.
11 *Gmelins Handbuch der anorganischen Chemie*, Vol. 61 A3, Verlag Chemie, Weinheim, 1977, p. 196.
12 Luppo-Cramer, *Kolloid-Z.*, 13 (1913) 180.
13 M. Kerker, *The Scattering of Light and Other Electromagnetic Radiation*, Academic, New York, 1969.
14 M. Kerker, *J. Opt. Soc. Am. B*, 2 (1985) 1327.
15 P.B. Johnson and R.W. Christy, *Phys. Rev. B*, 6 (1972) 4370.